

Actin polymerization kinetics, cap structure, and fluctuations

Dimitrios Vavylonis*, Qingbo Yang†, and Ben O’Shaughnessy**

Departments of *Chemical Engineering and †Physics, Columbia University, New York, NY 10027

Edited by Edward D. Korn, National Institutes of Health, Bethesda, MD, and approved April 28, 2005 (received for review February 19, 2005)

Polymerization of actin proteins into dynamic structures is essential to eukaryotic cell life, motivating many *in vitro* experiments measuring polymerization kinetics of individual filaments. Here, we model these kinetics, accounting for all relevant steps revealed by experiment: polymerization, depolymerization, random ATP hydrolysis, and release of phosphate (P_i). We relate filament growth rates to the dynamics of ATP-actin and ADP- P_i -actin caps that develop at filament ends. At the critical concentration of the barbed end, c_{crit} , we find a short ATP cap and a long fluctuation-stabilized ADP- P_i cap. We show that growth rates and the critical concentration at the barbed end are intimately related to cap structure and dynamics. Fluctuations in filament lengths are described by the length diffusion coefficient, D . Recently Fujiwara *et al.* [Fujiwara, I., Takahashi, S., Takaduma, H., Funatsu, T. & Ishiwata, S. (2002) *Nat. Cell Biol.* 4, 666–673] and Kuhn and Pollard [Kuhn, J. & Pollard, T. D. (2005) *Biophys. J.* 88, 1387–1402] observed large length fluctuations slightly above c_{crit} , provoking speculation that growth may proceed by oligomeric rather than monomeric on-off events. For the single-monomer growth process, we find that D exhibits a pronounced peak below c_{crit} , due to filaments alternating between capped and uncapped states, a mild version of the dynamic instability of microtubules. Fluctuations just above c_{crit} are enhanced but much smaller than those reported experimentally. Future measurements of D as a function of concentration can help identify the origin of the observed fluctuations.

ATP cap | length diffusivity | modeling | critical concentration

The tendency of actin protein to spontaneously polymerize into rapidly growing filaments is fundamental to the life of eukaryotic cells. Cell motility (1, 2), cell division (3), and endocytosis (4) are examples of processes exploiting the dynamic character of actin structures composed of filaments. The regulation of filament growth processes leads to well-defined structures and coordinated function. For example, in combination with branching, capping, and depolymerizing proteins, actin self-assembles into controlled dynamic cross-linked networks forming the dynamic core of lamellipodia (2).

These complex cellular actin-based systems exhibit multiple superposed mechanisms. A large body of *in vitro* work has sought to unravel these mechanisms and pin down rate constants for the constituent processes in purified systems (5). An important class of experiments entails measuring growth rate at one end by microscopy (6–9) or by bulk spectroscopic methods (10–16) as a function of actin monomer concentration. From these and other *in vitro* studies using various labeling techniques, the following picture has emerged of filament growth kinetics in the presence of ATP (see Fig. 1). (i) Monomers are added to a growing filament end as ATP-actin. (ii) Rapidly, the ATP is then hydrolyzed to ADP and phosphate (P_i), both remaining bound to the monomer host (ADP- P_i -actin) (10, 14, 17–22). A rate of 0.3 s^{-1} was reported in ref. 22 in the presence of Mg, assuming random hydrolysis uninfluenced by neighboring monomers. (iii) After a long delay, P_i release into solution occurs, generating ADP-actin (23–25). Reported release rates are in the range of 0.002 to 0.006 s^{-1} (23–26).

A typical filament in a growth rate experiment is thousands of monomer units (mon) in length and thus consists mainly of ADP-

actin. Hence, the picture that emerges is of a long ADP-actin filament with a complex three-state “cap” region at the filament end (5) (see Fig. 1). A major goal of this work is to establish the composition and kinetics of the cap and how these determine growth rates and measurable length fluctuations. The monomer composition is important in the context of cellular processes where it is thought to regulate actin-binding proteins in a timely and spatially organized way (2). For example, it has been suggested that rates of branching generated by the Arp2/3 protein complex and/or debranching processes may depend on which of the following three monomer species is involved: ATP-actin, ADP- P_i -actin, or ADP-actin (7, 26, 27). P_i release has been proposed to act as a timer for the action of the depolymerizing/severing protein ADF/cofilin, which preferentially attacks ADP-actin (2).

Our aim in this work is to establish theoretically the quantitative implications of the currently held picture of actin polymerization. Previous theoretical works addressed growth rates before the important process of P_i release was established (28–30). To our knowledge, to date, there has been no theoretical analysis of single filament non-steady-state growth rates rigorously accounting for the processes (i)–(iii) above. A recent theoretical work (31) has addressed steady-state filament compositions.

The cap has important consequences for the growth rate j as a function of ATP-actin concentration, c . Measured $j(c)$ curves, such as those in Fig. 5, are strikingly nonlinear in the region near the concentration where growth rate vanishes (16, 32). These curves become almost linear in excess P_i studies, where presumably the ADP-actin species is no longer involved (16). The complexity of the cap structure and dynamics also underlies the values of the critical concentration c_{crit} at the fast-growing “barbed” end and slow-growing “pointed” end of the polar actin filament (c_{crit} denotes the concentration where mean growth rate at one end vanishes). It is well known that in general these critical concentrations are different because detailed balance cannot be invoked for these nonequilibrium polymers (30). Our work explores how these differences are related to cap structure.

The major experimental focus has been mean growth rates, $j(c)$. However, equally revealing are fluctuations about the mean whose measurement can expose features of the dynamical processes occurring at filament ends unavailable from $j(c)$. These fluctuations are characterized by a “length diffusivity” D measuring the spread in filament lengths (see Fig. 1*b*) similarly to simple 1D Fickian diffusion: after time t , the root mean square fluctuation in filament length is $(2Dt)^{1/2}$ about the mean value $j(c)t$. By using single-filament microscopy, Fujiwara *et al.* (8) and Kuhn and Pollard (9) recently measured unexpectedly high values of this diffusivity near steady-state conditions, $D \approx 30 \text{ mon}^2/\text{s}$. This value should be compared with what would be expected of an equilibrium polymerization involving the measured on/off rates of order $1 \text{ mon}/\text{s}$, which would lead to $D \approx 1 \text{ mon}^2/\text{s}$ (8, 30, 33, 34). A number of

This paper was submitted directly (Track II) to the PNAS office.

Abbreviations: MC, Monte Carlo; mon, monomers.

*To whom correspondence should be addressed at: Department of Chemical Engineering, Columbia University, 500 West 120th Street, New York, NY 10027. E-mail: bo8@columbia.edu.

© 2005 by The National Academy of Sciences of the USA

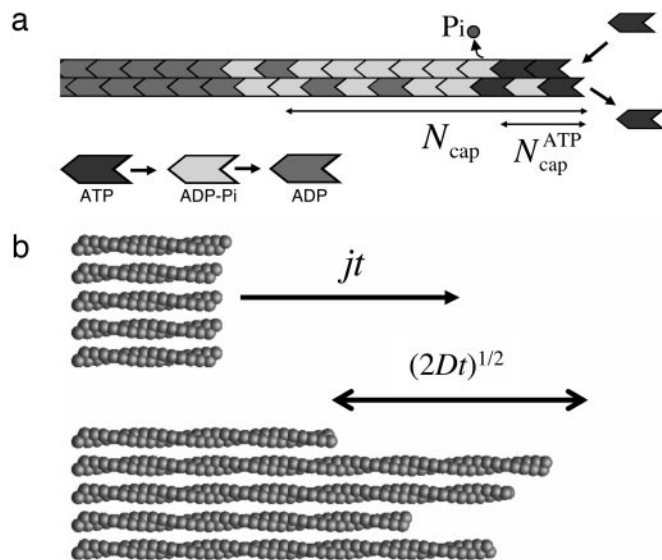


Fig. 1. Actin cap structure and growth kinetics. (a) Schematic of the three-species cap at the barbed end of a long actin filament. Near the critical concentration we find a fluctuation-induced cap of $N_{\text{cap}} \approx 25$ monomers, with a short ATP-actin component, $N_{\text{cap}}^{\text{ATP}}$ of order one. (b) Mean growth rate and fluctuations: in time t the average number of monomers added to a filament end is jt , with a spread of $(2Dt)^{1/2}$ about this value.

possible explanations were proposed. (i) Fluctuations arise from “dynamic instability” due to stochastic cap loss episodes. This phenomenon would be a far milder version of the “catastrophes” in microtubule polymerization (8, 35). (ii) Filament polymerization proceeds by addition and subtraction of oligomeric actin segment (8, 35); such kinetics would constitute a radical departure from the accepted picture of filament growth kinetics involving single monomer addition events. (iii) Growth involves extra stochastic events such as short pauses possibly originating in filament–surface attachments (9). (iv) Enhanced fluctuations result from an artifact due to monomer labeling (36). (v) These observed fluctuations result from experimental error in filament length measurements (9). A major focus of this work is to calculate the concentration-dependent length diffusivity, $D(c)$, assuming that the standard monomer-by-monomer addition picture is valid. We will see that large D values are realized below c_{crit} ; just above the critical concentration fluctuations are enhanced, although much less than the experimental values.

We consider the initial condition where long preformed ADP-actin seeds are exposed initially to a buffer of fixed actin concentration c and excess ATP. Thus, for a given c value, a filament consists of a very long ADP-actin core at the end of which lies a complex steady-state (but fluctuating) ATP-actin/ADP- P_i -actin cap. Our analysis emphasizes the barbed end, with the pointed end assumed blocked. Our results apply to very dilute filaments where only ATP-actin is assumed to add to filaments because (i) free monomers bind ATP more strongly than ADP (37) and (ii) depolymerized ADP-actin or ADP- P_i -actin has enough time to exchange its nucleotide for ATP before repolymerization. An important issue is the nature of the ATP hydrolysis mechanism: the experiments of refs. 20 and 21 support a random mechanism, although others have suggested a cooperative vectorial mechanism occurring at the interface between ADP- P_i -actin and ATP-actin with rate 13.6 s^{-1} (19, 28). In this work, random hydrolysis is assumed throughout.

Parameter Values and Mathematical Methods

One of the major aims of this work is to identify qualitative, but experimentally measurable, features of the growth kinetics that are

Table 1. Values of barbed end rate constants used in this work, appropriate for solutions of 50 mM KCl and 1 mM MgCl_2

k_T^+ , $\mu\text{M}^{-1}\cdot\text{s}^{-1}$	11.6*
v_T^-	1.4*
v_P^-	1.1†
v_D^-	7.2*
r_H	0.3‡
r_{P_i}	0.004§

Units are s^{-1} unless otherwise indicated.

*From ref. 6.

†Assigned; at present, there is no direct measurement of v_P^- , but $j(c)$ measurements with excess P_i (16) show the sum of the ADP- P_i -actin off rates at both ends together is a few times smaller than v_D^- .

‡From ref. 22.

§From refs. 23–26.

independent of the precise values of rate constants, because the latter depend on experimental conditions such as ionic strength (38) and the values themselves are often controversial. The parameter values we use are shown in Table 1, in which k_T^+ is the polymerization rate constant of ATP-actin, and v_T^- , v_D^- , and v_P^- are the depolymerization rates of ATP-actin, ADP-actin, and ADP- P_i -actin, respectively. The rates of ATP hydrolysis and P_i release (both assumed irreversible) are r_H and r_{P_i} , respectively. In addition, we will explore the effects of changing some of these parameter values. Because the monomer at the tip makes bonds with the two nearest neighbors, each belonging to a different protofilament, one expects that rate constants also may depend on the state of neighbors. Here, however, we study the simplest “one-body” model, assuming that on/off rates depend only on the attaching/detaching species (6) and that hydrolysis and P_i release rates are uniform along the filament. The influence of “many-body” effects will be discussed briefly below.

To calculate filament growth kinetics and composition, one is faced with the formidable task of obtaining the steady-state probability distribution of all possible actin monomer sequences along the filament; there are three possible states per monomer, so for filaments of N units long 3^N coupled equations must be solved. We have managed, however, to obtain a solution for the mean elongation rate $j(c)$ by projecting the full system of 3^N equations onto a set of just 3 exact equations for the return probabilities ψ_t^T , ψ_t^P , and ψ_t^D . These are the probabilities that a given monomer that was polymerized at $t = 0$ is again at the tip at time t as ATP-actin, ADP- P_i -actin, or ADP-actin, respectively.

The outline of our method is as follows. For $j < 0$ the growth rate is related to the return probabilities by $j = v_D^- p_{\text{core}}$, where $p_{\text{core}} = 1 - \int_0^\infty dt (\psi_t^D + \psi_t^P + \psi_t^T)$ is the probability of exposure of the ADP-actin core at the tip. For $j > 0$, the relation is $j = k_T^+ c - \int_0^\infty dt F_t$, where $F_t \equiv \psi_t^T v_T^- + \psi_t^P v_P^- + \psi_t^D v_D^-$ is the mean depolymerization rate at time t of a monomer that added to the tip at $t = 0$. The integral of F_t is the total depolymerization rate of added monomers. In *Supporting Material*, which is published as supporting information on the PNAS web site, we present the dynamical equations obeyed by the return probabilities, from which we obtained a closed recursion relation for the Laplace transform of F_t , namely f_E . This recursion relation relates f_E to f_{E+r_H} and $f_{E+r_{P_i}}$. With boundary condition $f_E \rightarrow 0$ as $E \rightarrow \infty$, we started from large E values and evolved this equation numerically toward $E = 0$ to obtain $f_0 \equiv \int_0^\infty dt F_t$. Given f_0 , the time integrals of the return probabilities then were obtained directly from the dynamical equations, and j was thereby determined.

The above analytically based method does not generate cap sizes and length diffusivities. To calculate these quantities and also to test the validity of the analytical method, we have simulated the stochastic tip dynamics employing the kinetic Monte Carlo (MC) method known as the BKL (39) or Gillespie (40) algorithm to

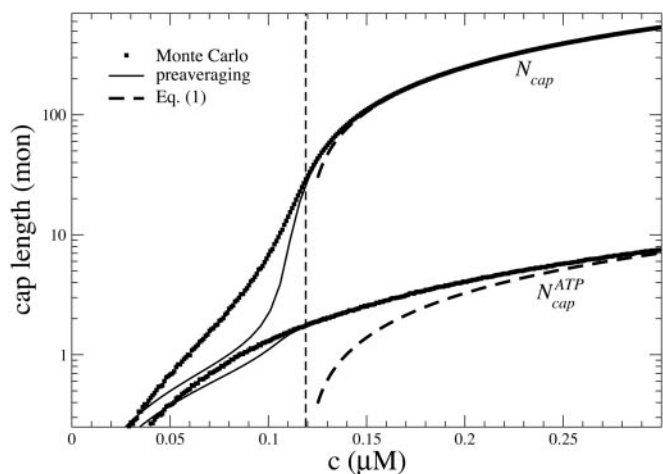


Fig. 2. Total cap length $N_{\text{cap}}(c)$ and ATP-actin cap length $N_{\text{cap}}^{\text{ATP}}(c)$ at barbed end. Parameters are from Table 1. Squares indicate MC results. Dashed lines refer to Eq. 1. Solid lines indicate preaveraging approximation. Vertical dashed line indicates $c_{\text{crit}} = 0.119 \mu\text{M}$.

evolve the state of a filament tip in time and to calculate its mean growth rate. Each step of the algorithm entails updating time by an amount depending on the rate and number of possible future events, namely polymerization/depolymerization, hydrolysis, and P_i release. Excellent agreement is found between MC results and the numerical solutions of our closed equations for the growth rate (see Fig. 3 *Inset*).

Our analytical method is exact and avoids preaveraging, an approximation where the joint probability of a given filament nucleotide sequence is approximated as a product of probabilities for individual actin subunits. This approximation neglects correlations between units. To assess the accuracy of this scheme, we compared our results for cap size and growth rate with those obtained by using preaveraging (see *Supporting Material* for details). Preaveraging has been used in other theoretical studies of actin polymerization such as ref. 31 to study steady state and ref. 32 to study growth rates.

Cap Structure and the Importance of Fluctuations

By using the parameters of Table 1, in Fig. 2 we present MC results for (i) the total cap size, N_{cap} , namely the mean total number of ATP-actin and ADP- P_i -actin subunits at the barbed end, as a function of concentration, and (ii) the number of ATP-actin cap subunits, $N_{\text{cap}}^{\text{ATP}}$. Fig. 2 shows that both caps become large for large concentrations. This behavior is easy to understand. Consider, for example, the ATP cap: when polymerization rates exceed both the hydrolysis rate r_{H} and the depolymerization rates, the interface between ADP- P_i -actin and ATP-actin follows the growing tip with a lag of $j(c)/r_{\text{H}}$ monomers. Thus,

$$N_{\text{cap}}^{\text{ATP}} = j(c)/r_{\text{H}}, \quad N_{\text{cap}}^{\text{ADPP}_i} = j(c)/r_{\text{P}_i} \quad (c \gg c_{\text{crit}}). \quad [1]$$

Here, the number of ADP- P_i subunits, $N_{\text{cap}}^{\text{ADPP}_i}$, is found by using similar reasoning as for $N_{\text{cap}}^{\text{ATP}}$. The validity of Eq. 1 for large concentrations is verified against MC data in Fig. 2.

The striking feature of Fig. 2 is that the total cap remains long even below the critical concentration of the barbed end, being 25 units at c_{crit} and remaining larger than unity down to $c \approx c_{\text{crit}}/2$. One might naively have guessed that below c_{crit} there would be no cap at all, because the filament is shrinking into its ADP core. (Indeed, the absence of a cap would also be suggested by Eq. 1 if one were to extend its validity down to c_{crit} where $j = 0$.) This reasoning is, however, invalid because it neglects fluctuations due to randomness of monomer addition/subtraction.

To understand why fluctuations lead to long caps, consider the length changes of the cap only, excluding changes in the ADP-actin core length. Just below the critical concentration, the tip of a typical long cap has a net shrinkage rate (33, 34), $v_{\text{cap}}(c)$. This value is a weighted average of rates, summed over all possible states of the short ATP-actin segment on top of the long ADP- P_i -actin segment. Because v_{cap} is a smooth function of c , it can be Taylor-expanded near the critical concentration and expressed as $v_{\text{cap}} = k_{\text{eff}}^+(c - c_{\text{crit}})$, where k_{eff}^+ is an effective on rate constant, different from k_{T}^+ . Now superposed on this average shrinkage, the cap tip also performs a random walk in cap length space, described by a diffusivity $D_{\text{cap}}(c)$ (8, 33, 34), also an average over the states of the short ATP cap. (D_{cap} is in fact the short-time diffusivity of the entire filament; see discussion below.) For small times, diffusivity dominates and of order $(2D_{\text{cap}}t)^{1/2}$ units add to or subtract from the cap. For times less than the cap turnover time t_{cap} , this number is much bigger than the number of units wiped out by coherent shrinkage, $v_{\text{cap}}t_{\text{cap}}$. The cap lifetime t_{cap} is the time when the shrinkage just catches up, $v_{\text{cap}}t_{\text{cap}} \approx (2D_{\text{cap}}t_{\text{cap}})^{1/2}$. Hence, the approximate dependence of cap length on concentration is

$$N_{\text{cap}} = v_{\text{cap}}t_{\text{cap}} \approx 2D_{\text{cap}}/[k_{\text{eff}}^+(c_{\text{crit}} - c)], \quad (c < c_{\text{crit}}), \quad [2]$$

which indeed becomes large as c_{crit} is approached from below.

In summary, even though on average below c_{crit} no ATP-actin monomers are being added to the tip, fluctuations in addition/subtraction rates allow a cap to grow to length $(2D_{\text{cap}}t_{\text{cap}})^{1/2}$ because the cap length diffusivity is dominant for times less than t_{cap} . Now because P_i release is very slow, for simplicity in deriving Eq. 2 we assumed the release rate was zero, $r_{\text{P}_i} = 0$. However, the result of Eq. 2 is valid even for a nonzero r_{P_i} except for concentrations so close to c_{crit} that the cap turnover time exceeds the P_i release time. In this inner region, diffusion is only able to grow the cap for a time of order $r_{\text{P}_i}^{-1}$ before P_i release intervenes. The maximum possible cap length, attained very close to c_{crit} , is thus,

$$N_{\text{cap}}^{\text{crit}} \approx [2D_{\text{cap}}(c_{\text{crit}})/r_{\text{P}_i}]^{1/2}. \quad [3]$$

Eq. 2 is valid until N_{cap} reaches this bound.

These arguments explain the origin of the long caps below c_{crit} . To make a quantitative comparison of Eqs. 2 and 3 to the numerics of Fig. 2, the values of D_{cap} and v_{cap} must be determined. Now because for our parameter set v_{T}^- and v_{P}^- have similar values (see Table 1), an estimate can be obtained by considering the special case where $v_{\text{T}}^- = v_{\text{P}}^-$ (identical ATP-actin and ADP- P_i -actin). This case is convenient because D_{cap} and v_{cap} can be calculated exactly; the cap has just one monomer species, so $k_{\text{eff}}^+ = k_{\text{T}}^+$, and $D_{\text{cap}}(c_{\text{crit}}) = (k_{\text{T}}^+c_{\text{crit}} + v_{\text{T}}^-)/2$ (8, 33, 34). By using the values of Table 1 in these expressions and in Eq. 3 gives $N_{\text{cap}}^{\text{crit}} \approx 26$, of the same order as the numerics of Fig. 2.

Finally, note that the preaveraging method shown in Fig. 2 is an excellent approximation in regions where fluctuations are unimportant (very large or very small c), producing almost identical results to MC. However, below c_{crit} it considerably underestimates cap lengths. This error results from the preaveraged treatment of fluctuations.

Mean Growth Rate, $j(c)$

How is the behavior of the average rate of growth $j(c)$ correlated to cap structure and dynamics? The lowest curve of Fig. 3 shows numerical results for barbed end growth, using identical parameters to those of Fig. 2. A noticeable feature is that the slopes are very different above and below the critical concentration of the barbed end. This difference directly reflects the cap structure just discussed, as follows. For $c \gg c_{\text{crit}}$ the ATP-actin segment is long and hides the remaining ADP- P_i -actin portion of the cap, so $j \approx k_{\text{T}}^+c -$

(50) experiments examining ATP/ADP-P_i differences for filamentous actin.

If we adhere to the assumption that the growth mechanisms as previously outlined apply to both ends, we then are led to the following prediction: the values of c_{crit} for ATP-actin at both ends will be only weakly affected by the presence of excess P_i (provided ionic conditions are strictly unchanged). This prediction follows because the binding of P_i to ADP-actin segments is almost irrelevant because these are rarely exposed at the tip due to long caps at c_{crit} . Indeed, for the barbed end no significant shift has been observed in the presence of P_i (16, 44–46). For the pointed end, however, a reduction of c_{crit} has been reported in the presence of P_i and barbed end capping proteins (16, 44–46). This observation cannot be explained within the present framework and suggests possibility (ii). Future experiments will hopefully settle this important issue.

Conclusions

In this work, filament growth rates $j(c)$ and their fluctuations, as measured by the diffusivity $D(c)$, were calculated as functions of ATP-actin concentration c . This work presents a rigorous calculation of these quantities accounting for all known basic mechanisms. Pantaloni *et al.* (28, 29) studied $j(c)$ at the barbed end in a work before the mechanism of P_i release was discovered. Infinitely fast P_i release and vectorial hydrolysis were assumed. Given the data available at that time, to explain the sharp change in slope of $j(c)$ at c_{crit} (see, e.g., Fig. 5), they further assumed (i) strong three-body ATP-actin/ADP-actin interactions that lead to stable short ATP-actin caps, and (ii) zero hydrolysis rate of the nucleotide bound to the terminal monomer. In our work, the origin of the sharp change

in slope is precisely the fact that P_i release is slow, similar to an earlier model of microtubule polymerization (51).

Recently, Bindschadler *et al.* (31) studied the composition of actin filaments accounting for all three actin species at steady state. We have examined the preaveraging approximation used in their work and showed that it leads to very accurate $j(c)$ curves, but the cap lengths are underestimated below c_{crit} .

Here, we have addressed random ATP hydrolysis only. Further work is needed to analyze the implications of the vectorial hydrolysis suggested by refs. 19 and 28. We showed that for random hydrolysis $j(c)$ is linear far above the critical concentration. Growth rate experiments for both ends together in the absence of KCl have exhibited nonlinearities up to $c = 10 \mu\text{M}$, far above the critical concentration of the barbed end, which is $1 \mu\text{M}$ under these conditions (10, 11). In refs. 10 and 28, this observation was attributed to vectorial hydrolysis at the barbed end, whereas in ref. 6 this behavior was assigned to the nonlinear contribution of the pointed end whose critical concentration is $\approx 5 \mu\text{M}$ under the same conditions.

Perhaps our most interesting finding is that the long time diffusivity D_{∞} has a large peak below the critical concentration c_{crit} of the barbed end, followed by a sharp drop in a narrow range above c_{crit} . This conclusion is quite general, and its origin is the smallness of the P_i release rate and the large value of the off rate of ADP-actin at the barbed end. Future measurements of length diffusivities over a range of concentrations promise to provide new information and insight on the fundamentals of actin polymerization.

We thank Ikuko Fujiwara, Jeffrey Kuhn, and Thomas Pollard for stimulating discussions. This work was supported by Petroleum Research Fund Grant 33944-AC7 and National Science Foundation Grant CHE-00-91460.

- Bray, D. (2000) *Cell Movements. From Molecules to Motility* (Garland, New York), 2nd Ed.
- Pollard, T. D. & Borisy, G. G. (2003) *Cell* **112**, 453–465.
- Pelham, R. J. & Chang, F. (2002) *Nature* **419**, 82–86.
- Young, M. E., Cooper, J. A. & Bridgman, P. C. (2004) *J. Cell. Biol.* **166**, 629–635.
- Korn, E. D., Carlier, M.-F. & Pantaloni, D. (1987) *Science* **238**, 638–643.
- Pollard, T. D. (1986) *J. Cell Biol.* **103**, 2747–2754.
- Amann, K. J. & Pollard, T. D. (2001) *Proc. Natl. Acad. Sci. USA* **98**, 15009–15013.
- Fujiwara, I., Takahashi, S., Takaduma, H., Funatsu, T. & Ishiwata, S. (2002) *Nat. Cell Biol.* **4**, 666–673.
- Kuhn, J. & Pollard, T. D. (2005) *Biophys. J.* **88**, 1387–1402.
- Carlier, M.-F., Pantaloni, D. & Korn, E. D. (1984) *J. Biol. Chem.* **259**, 9983–9986.
- Carlier, M.-F., Pantaloni, D. & Korn, E. D. (1985) *J. Biol. Chem.* **260**, 6565–6571.
- Coué, M. & Korn, E. D. (1986) *J. Biol. Chem.* **261**, 1588–1593.
- Carlier, M.-F., Criquet, P., Pantaloni, D. & Korn, E. D. (1986) *J. Biol. Chem.* **261**, 2041–2050.
- Carlier, M.-F., Pantaloni, D. & Korn, E. D. (1986) *J. Biol. Chem.* **261**, 10785–10792.
- Weber, A., Northrop, J., Bishop, M. F., Ferrone, F. A. & Mooseker, M. S. (1987) *Biochemistry* **26**, 2537–2544.
- Carlier, M.-F. & Pantaloni, D. (1988) *J. Biol. Chem.* **263**, 817–825.
- Pardee, J. D. & Spudich, J. A. (1982) *J. Cell Biol.* **93**, 648–654.
- Pollard, T. D. & Weeds, A. G. (1984) *FEBS Lett.* **170**, 94–98.
- Carlier, M.-F., Pantaloni, D. & Korn, E. D. (1987) *J. Biol. Chem.* **262**, 3052–3059.
- Ohm, T. & Wegner, A. (1994) *Biochim. Biophys. Acta* **1208**, 8–14.
- Pieper, U. & Wegner, A. (1996) *Biochemistry* **35**, 4396–4402.
- Blanchoin, L. & Pollard, T. D. (2002) *Biochemistry* **41**, 597–602.
- Carlier, M.-F. & Pantaloni, D. (1986) *Biochemistry* **35**, 7789–7792.
- Carlier, M.-F. (1987) *Biochem. Biophys. Res. Commun.* **143**, 1069–1075.
- Melki, R., Fievez, S. & Carlier, M.-F. (1996) *Biochemistry* **35**, 12038–12045.
- Blanchoin, L., Pollard, T. D. & Mullins, R. D. (2000) *Curr. Biol.* **10**, 1273–1282.
- Ichetovkin, I., Grant, W. & Condeelis, J. (2002) *Curr. Biol.* **12**, 79–84.
- Pantaloni, D., Hill, T. L., Carlier, M. F. & Korn, E. D. (1985) *Proc. Natl. Acad. Sci. USA* **82**, 7207–7211.
- Hill, T. L. (1986) *Biophys. J.* **49**, 981–986.
- Hill, T. L. (1987) *Linear Aggregation Theory in Cell Biology* (Springer, New York).
- Bindschadler, M., Osborn, E. A., Dewey, C. F. J. & McGrath, J. L. (2004) *Biophys. J.* **86**, 2720–2739.
- Keiser, T., Schiller, A. & Wegner, A. (1986) *Biochemistry* **25**, 4899–4906.
- O’Shaughnessy, B. & Vavylonis, D. (2003) *Phys. Rev. Lett.* **90**, 118301.
- O’Shaughnessy, B. & Vavylonis, D. (2003) *Eur. Phys. J. E* **12**, 481–496.
- Littlefield, R. & Fowler, V. M. (2002) *Nat. Cell Biol.* **4**, E209–E210.
- Kudryasov, D. S., Phillips, M. & Reisler, E. (2004) *Biophys. J.* **87**, 1136–1145.
- Kinosian, H. J., Selden, L. A., Estes, J. E. & Gershman, L. C. (1993) *J. Biol. Chem.* **268**, 8683–8691.
- Drenckhahn, D. & Pollard, T. D. (1986) *J. Biol. Chem.* **261**, 12754–12758.
- Bortz, A. B., Kalos, M. H. & Lebowitz, J. L. (1975) *J. Comput. Phys.* **17**, 10–18.
- Gillespie, D. T. (1977) *J. Phys. Chem.* **81**, 2340–2361.
- Hill, T. L. & Chen, Y.-D. (1984) *Proc. Natl. Acad. Sci. USA* **81**, 5772–5776.
- Fisher, M. E. (1984) *J. Stat. Phys.* **34**, 667–729.
- Brenner, S. L. & Korn, E. D. (1983) *J. Biol. Chem.* **258**, 5013–5020.
- Rickard, J. E. & Sheterline, P. (1986) *J. Mol. Biol.* **191**, 273–280.
- Wanger, M. & Wegner, A. (1987) *Biochim. Biophys. Acta* **915**, 105–113.
- Weber, A., Pennise, C. R. & Fowler, V. M. (1999) *J. Biol. Chem.* **274**, 34637–34645.
- Carlier, M.-F., Pantaloni, D., Evans, J. A., Lambooy, P. K., Korn, E. D. & Webb, M. R. (1988) *FEBS Lett.* **235**, 211–214.
- Dickinson, R. B., Caro, L. & Purich, D. L. (2004) *Biophys. J.* **87**, 2838–2854.
- Otterbein, L. R., Graceffa, P. & Dominguez, R. (2001) *Science* **293**, 708–711.
- Belmont, L. D., Orlova, A., Drubin, D. G. & Egelman, E. H. (1999) *Proc. Natl. Acad. Sci. USA* **96**, 29–34.
- Hill, T. L. & Carlier, M.-F. (1983) *Proc. Natl. Acad. Sci. USA* **80**, 7234–7238.

SUPPORTING MATERIAL

A. Numerical Method for Growth Rates.

Here we describe the numerical method we used in the main text to calculate the growth rate curves of Figs. 3 and 4. Consider an ATP-actin monomer that polymerizes at the filament tip at time $t = 0$. We define the return probabilities ψ_t^T , ψ_t^P , and ψ_t^D to be the probability that this monomer is once again at the tip after time t as ATP-actin, ADP-Pi-actin, or ADP-actin, respectively. The total depolymerization rate of this monomer at time t is

$$F_t = v_{\bar{T}}\psi_t^T + v_{\bar{P}}\psi_t^P + v_{\bar{D}}\psi_t^D . \quad (1)$$

The dynamical equations obeyed by the return probabilities are

$$\begin{aligned} \frac{d}{dt}\psi_t^T &= -(k_{\bar{T}}^+c + v_{\bar{T}} + r_H)\psi_t^T + k_{\bar{T}}^+c \int_0^t dt' \psi_{t-t'}^T F_{t-t'} e^{-r_H(t-t')} , \\ \frac{d}{dt}\psi_t^P &= -(k_{\bar{T}}^+c + v_{\bar{P}} + r_{Pi})\psi_t^P + r_H\psi_t^T + k_{\bar{T}}^+c \int_0^t dt' \psi_{t-t'}^P F_{t-t'} e^{-r_{Pi}(t-t')} \\ &\quad + k_{\bar{T}}^+c \int_0^t dt' \psi_{t-t'}^T F_{t-t'} \frac{r_H}{r_{Pi} - r_H} \left(e^{-r_H(t-t')} - e^{-r_{Pi}(t-t')} \right) , \\ \frac{d}{dt}\psi_t^D &= -(k_{\bar{T}}^+c + v_{\bar{D}})\psi_t^D + r_{Pi}\psi_t^P + k_{\bar{T}}^+c \int_0^t dt' \psi_{t-t'}^D F_{t-t'} + k_{\bar{T}}^+c \int_0^t dt' \psi_{t-t'}^P F_{t-t'} \left(1 - e^{-r_{Pi}(t-t')} \right) \\ &\quad + k_{\bar{T}}^+c \int_0^t dt' \psi_{t-t'}^T F_{t-t'} \left(1 - \frac{r_{Pi}}{r_{Pi} - r_H} e^{-r_H(t-t')} + \frac{r_H}{r_{Pi} - r_H} e^{-r_{Pi}(t-t')} \right) . \end{aligned} \quad (2)$$

Here the non-integral terms on the right-hand sides represent change of tip status due to polymerization, depolymerization, hydrolysis, and phosphate release events at time t . The integral terms represent rates of reappearance of the monomer at the tip, weighted by factors accounting for the probability of hydrolysis or phosphate release during the time interval since the last appearance at the tip. For example, the first term on the right-hand side of the first equation represents the rate of change of the probability of finding the ATP-actin monomer at the tip due to (i) polymerization of another monomer on top of it, (ii) depolymerization of the monomer itself, or (iii) hydrolysis of the ATP nucleotide bound to the monomer at the tip. The integral term on the right-hand side represents reappearance events of the ATP-actin unit at the tip given that it got buried inside the filament due to a polymerization event at time t' , an event that occurred with rate $k_{\bar{T}}^+c$. Factor F represents the rate of reappearance of the buried monomer at the tip due to depolymerization of all the monomers that were added on top of it. The factor $e^{-r_H(t-t')}$ is the probability that the ATP-actin monomer in question is not hydrolyzed while being buried.

Now the filament growth rate is given by

$$j = \begin{cases} v_{\bar{D}} \left[1 - \int_0^\infty dt (\psi_t^D + \psi_t^P + \psi_t^T) \right] & (j < 0) \\ k_{\bar{T}}^+c - \int_0^\infty dt F_t & (j > 0) \end{cases} . \quad (3)$$

Carrying out a Laplace transformation, $t \rightarrow E$, $F_t \rightarrow f_E$, and $\psi_t \rightarrow \Psi_E$ one has from Eq. 3

$$j = \begin{cases} v_{\bar{D}} \left[1 - \Psi_0^D - \Psi_0^P - \Psi_0^T \right] & (j < 0) \\ k_{\bar{T}}^+c - f_0 & (j > 0) \end{cases} \quad (4)$$

while from Eq. 2 one obtains

$$\Psi_E^T = 1 / \left(E + v_{\bar{T}} + r_H + k_{\bar{T}}^+c(1 - f_{E+r_H}) \right) ,$$

$$\begin{aligned}\Psi_E^P &= \frac{r_H + k_T^+ c r_H (f_{E+r_H} - f_{E+r_{P_i}}) / (r_{P_i} - r_H)}{E + v_{\bar{P}} + r_{P_i} + k_T^+ c (1 - f_{E+r_{P_i}})} \Psi_E^T, \\ \Psi_E^D &= \frac{(r_{P_i} + k_T^+ c (f_E - f_{E+r_{P_i}})) \Psi_E^P + k_T^+ c (f_E - r_{P_i} f_{E+r_H} / (r_{P_i} - r_H) + r_H f_{E+r_{P_i}} / (r_{P_i} - r_H)) \Psi_E^T}{E + v_{\bar{D}} + k_T^+ c (1 - f_E)}\end{aligned}\quad (5)$$

Eliminating all Ψ in the Laplace transformation of Eq. 1 after using Eq. 5 one obtains the following recursive relationship involving the function f alone:

$$f_E = \mathcal{R}[f_{E+r_H}, f_{E+r_{P_i}}], \quad (6)$$

where

$$\mathcal{R}[f_{E+r_H}, f_{E+r_{P_i}}] = \frac{-b_1 + \sqrt{b_1^2 - 4b_2 b_0}}{2b_2}. \quad (7)$$

Here the symbols b_0 , b_1 , and b_2 are functions of E , f_{E+r_H} and $f_{E+r_{P_i}}$ as follows:

$$\begin{aligned}b_0 &= A_{0,2} E^2 + A_{0,1} E + A_{0,0}, \\ b_1 &= A_{1,3} E^3 + A_{1,2} E^2 + A_{1,1} E + A_{1,0}, \\ b_2 &= A_{2,2} E^2 + A_{2,1} E + A_{2,0},\end{aligned}\quad (8)$$

where

$$\begin{aligned}A_{0,2} &= -(r_H - r_{P_i}) v_{\bar{T}} k_T^+ c, \\ A_{0,1} &= (v_{\bar{D}} r_H - r_{P_i} v_{\bar{T}} + r_H (-v_{\bar{P}} + v_{\bar{T}})) (k_T^+ c)^2 f_{E+r_{P_i}} + (r_H v_{\bar{P}} - v_{\bar{D}} r_{P_i}) (k_T^+ c)^2 f_{E+r_H} \\ &\quad - (r_H - r_{P_i}) k_T^+ c (r_H v_{\bar{P}} + v_{\bar{T}} (v_{\bar{D}} + v_{\bar{P}} + r_{P_i} + 2k_T^+ c)), \\ A_{0,0} &= -v_{\bar{D}} (r_H - r_{P_i}) (k_T^+ c)^3 f_{E+r_{P_i}} f_{E+r_H} \\ &\quad - (r_H (v_{\bar{P}} - v_{\bar{T}}) + r_{P_i} v_{\bar{T}}) k_T^+ c + v_{\bar{D}} ((r_H)^2 - r_{P_i} v_{\bar{T}} + r_H (-r_{P_i} + v_{\bar{T}} + k_T^+ c)) (k_T^+ c)^2 f_{E+r_{P_i}} \\ &\quad + (r_H v_{\bar{P}} k_T^+ c + v_{\bar{D}} (r_H (v_{\bar{P}} + r_{P_i}) - r_{P_i} (v_{\bar{P}} + r_{P_i} + k_T^+ c))) (k_T^+ c)^2 f_{E+r_H} \\ &\quad - (r_H - r_{P_i}) k_T^+ c (k_T^+ c (r_H v_{\bar{P}} + v_{\bar{T}} (v_{\bar{P}} + r_{P_i} + k_T^+ c)) + v_{\bar{D}} (r_H (v_{\bar{P}} + r_{P_i}) + v_{\bar{T}} (v_{\bar{P}} + r_{P_i} + k_T^+ c))), \\ A_{1,3} &= r_H - r_{P_i}, \\ A_{1,2} &= -(r_H - r_{P_i}) k_T^+ c (f_{E+r_{P_i}} + f_{E+r_H}) + (r_H - r_{P_i}) (v_{\bar{D}} + r_H + v_{\bar{P}} + r_{P_i} + v_{\bar{T}} + 3k_T^+ c), \\ A_{1,1} &= (r_H - r_{P_i}) (k_T^+ c)^2 f_{E+r_{P_i}} f_{E+r_H} - (r_H - r_{P_i}) (v_{\bar{D}} + r_H + v_{\bar{T}} + 2k_T^+ c) k_T^+ c f_{E+r_{P_i}} \\ &\quad - (r_H - r_{P_i}) (v_{\bar{D}} + v_{\bar{P}} + r_{P_i} + 2k_T^+ c) k_T^+ c f_{E+r_H} \\ &\quad + (r_H - r_{P_i}) (v_{\bar{P}} v_{\bar{T}} + r_{P_i} v_{\bar{T}} + 2v_{\bar{P}} k_T^+ c + 2r_{P_i} k_T^+ c + 3v_{\bar{T}} k_T^+ c + 3(k_T^+ c)^2 \\ &\quad \quad + v_{\bar{D}} (r_H + v_{\bar{P}} + r_{P_i} + v_{\bar{T}} + k_T^+ c) + r_H (v_{\bar{P}} + r_{P_i} + 2k_T^+ c)), \\ A_{1,0} &= (r_H - r_{P_i}) (v_{\bar{D}} + k_T^+ c) (k_T^+ c)^2 f_{E+r_{P_i}} f_{E+r_H} \\ &\quad + (-v_{\bar{D}} (r_H^2 - r_{P_i} v_{\bar{T}} + r_H (-r_{P_i} + v_{\bar{T}} + k_T^+ c)) \\ &\quad \quad + k_T^+ c (-r_H^2 + r_H (v_{\bar{P}} + r_{P_i} - 2v_{\bar{T}} - k_T^+ c) + r_{P_i} (2v_{\bar{T}} + k_T^+ c))) k_T^+ c f_{E+r_{P_i}} \\ &\quad + (v_{\bar{D}} (-r_H (v_{\bar{P}} + r_{P_i}) + r_{P_i} (v_{\bar{P}} + r_{P_i} + k_T^+ c)) \\ &\quad \quad + k_T^+ c (r_{P_i} (v_{\bar{P}} + r_{P_i} + k_T^+ c) - r_H (2v_{\bar{P}} + r_{P_i} + k_T^+ c))) k_T^+ c f_{E+r_H} \\ &\quad + (r_H - r_{P_i}) (v_{\bar{D}} (r_H (v_{\bar{P}} + r_{P_i}) + v_{\bar{T}} (v_{\bar{P}} + r_{P_i} + k_T^+ c)) \\ &\quad \quad + k_T^+ c (r_H (2v_{\bar{P}} + r_{P_i} + k_T^+ c) + (v_{\bar{P}} + r_{P_i} + k_T^+ c) (2v_{\bar{T}} + k_T^+ c))), \\ A_{2,2} &= r_{P_i} - r_H, \\ A_{2,1} &= (r_H - r_{P_i}) k_T^+ c (f_{E+r_{P_i}} + f_{E+r_H}) - (r_H - r_{P_i}) (r_H + v_{\bar{P}} + r_{P_i} + v_{\bar{T}} + 2k_T^+ c), \\ A_{2,0} &= -(r_H - r_{P_i}) (k_T^+ c)^2 f_{E+r_{P_i}} f_{E+r_H} + (r_H - r_{P_i}) (r_H + v_{\bar{T}} + k_T^+ c) k_T^+ c f_{E+r_{P_i}} \\ &\quad + (r_H - r_{P_i}) (v_{\bar{P}} + r_{P_i} + k_T^+ c) k_T^+ c f_{E+r_H} - (r_H - r_{P_i}) (v_{\bar{P}} + r_{P_i} + k_T^+ c) (r_H + v_{\bar{T}} + k_T^+ c).\end{aligned}\quad (9)$$

We remark that Eq. 7 is the solution of a quadratic equation; which of the two solutions of the quadratic is meaningful is easily checked by demanding $f < 1$ in the $E \rightarrow \infty$ limit.

Now for any given monomer concentration c , with the boundary condition $f_E \rightarrow 0$ as $E \rightarrow \infty$, we started from a large enough E value and evolved Eq. 6 towards $E = 0$ to obtain f_0 , $f_{r_{\text{Pi}}}$, and $f_{r_{\text{H}}}$. Substituting these values in Eq. 5 we further obtained Ψ_0^{T} , Ψ_0^{P} , and Ψ_0^{D} . Thus, given f_0 , Ψ_0^{T} , Ψ_0^{P} , and Ψ_0^{D} we evaluated $j(c)$ using Eq. 4. It was shown that this method converges to a unique solution provided one starts the evolution from large enough E , retaining a sufficient number of significant digits.

B. Preaveraging Approximation: Calculation of Growth Rates.

Here we present the method we used to calculate cap sizes and growth rates based on a preaveraging approximation. As discussed in the main text, compared with the exact calculations, this method gives different results for the cap size below c_{crit} , but provides very good approximations to growth rates. We denote $\phi_{\text{T}}(n)$, $\phi_{\text{P}}(n)$, and $\phi_{\text{D}}(n)$ the probability that the n^{th} monomer away from the tip binds ATP, ADP-Pi, or ADP, respectively. Consider first the tip, i. e. $n = 1$. One has (1)

$$\frac{d}{dt}\phi_{\text{T}}(1) = k_{\text{T}}^+c[\phi_{\text{P}}(1) + \phi_{\text{D}}(1)] + [v_{\text{P}}^- \phi_{\text{P}}(1) + v_{\text{D}}^- \phi_{\text{D}}(1)]\phi_{\text{T}}(2) - v_{\text{T}}^-[\phi_{\text{P}}(2) + \phi_{\text{D}}(2)]\phi_{\text{T}}(1) - r_{\text{H}}\phi_{\text{T}}(1) . \quad (10)$$

The first term on the right-hand side represents change of tip status into ATP-actin due to polymerization of ATP-actin at an ADP-Pi-actin or ADP-actin tip. The second term represents change of tip status into ATP-actin due to (i) depolymerization of ADP-Pi-actin or ADP-actin at $n = 1$, and (ii) exposure of ATP-actin, previously buried at position $n = 2$. Within the preaveraging approximation, the joint probability of ADP at $n = 1$ and simultaneously ATP at $n = 2$, for example, is approximated as a product of probabilities: $\phi_{\text{DT}}(1, 2) \approx \phi_{\text{D}}(1)\phi_{\text{T}}(2)$ in Eq. 10. Similarly, the third term on the right-hand side represents depolymerization of ATP-actin while the last term is change due to hydrolysis.

For ADP-Pi-actin one has similarly

$$\frac{d}{dt}\phi_{\text{P}}(1) = [v_{\text{T}}^- \phi_{\text{T}}(1) + v_{\text{D}}^- \phi_{\text{D}}(1)]\phi_{\text{P}}(2) - \left\{ v_{\text{P}}^- [\phi_{\text{T}}(2) + \phi_{\text{D}}(2)] + k_{\text{T}}^+c + r_{\text{Pi}} \right\} \phi_{\text{P}}(1) + r_{\text{H}}\phi_{\text{T}}(1) . \quad (11)$$

The analogous equations for $n > 1$ are (1)

$$\begin{aligned} \frac{d}{dt}\phi_{\text{T}}(n) &= k_{\text{T}}^+c[\phi_{\text{T}}(n-1) - \phi_{\text{T}}(n)] + [v_{\text{T}}^- \phi_{\text{T}}(1) + v_{\text{D}}^- \phi_{\text{D}}(1) + v_{\text{P}}^- \phi_{\text{P}}(1)][\phi_{\text{T}}(n+1) - \phi_{\text{T}}(n)] - r_{\text{H}}\phi_{\text{T}}(n) \\ \frac{d}{dt}\phi_{\text{P}}(n) &= k_{\text{T}}^+c[\phi_{\text{P}}(n-1) - \phi_{\text{P}}(n)] + [v_{\text{T}}^- \phi_{\text{T}}(1) + v_{\text{D}}^- \phi_{\text{D}}(1) + v_{\text{P}}^- \phi_{\text{P}}(1)][\phi_{\text{P}}(n+1) - \phi_{\text{P}}(n)] \\ &+ r_{\text{H}}\phi_{\text{T}}(n) - r_{\text{Pi}}\phi_{\text{P}}(n) \quad (n > 1) \end{aligned} \quad (12)$$

The rate of change of the ADP-actin probabilities are determined from $\phi_{\text{T}}(n) + \phi_{\text{P}}(n) + \phi_{\text{D}}(n) = 1$. Starting from an arbitrary nucleotide profile and using long filaments, we evolved numerically Eqs. 10-12 for a long enough time to allow the profile to reach its steady state [note that an analytical solution is also possible since Eq. 12 is linear, except for the tip terms (1)]. The growth rate and the cap size were calculated from

$$N_{\text{cap}} = \sum_{n=1}^{\infty} \phi_{\text{T}}(n) + \phi_{\text{P}}(n), \quad N_{\text{cap}}^{\text{ATP}} = \sum_{n=1}^{\infty} \phi_{\text{T}}(n), \quad j = k_{\text{T}}^+c - v_{\text{T}}^- \phi_{\text{T}}(1) - v_{\text{P}}^- \phi_{\text{P}}(1) - v_{\text{D}}^- \phi_{\text{D}}(1) . \quad (13)$$

C. Analytical Calculation of Length Diffusivity as a Function of Concentration.

Here we prove that $D_\infty(c)$ in Fig. 6 has a sawtooth shape in the special case $v_{\text{P}}^- = v_{\text{T}}^-$ and $r_{\text{Pi}} \rightarrow 0$. Consider first shrinking barbed ends, $c < c_{\text{crit}}$. For long times, $t \gg t_{\text{cap}}$, apart from fluctuations in the size of the steady-state ATP/ADP-Pi cap, fluctuations in tip displacement are due to fluctuations in how far the ADP core has shrunk. Let us call $u(\tau|t)$ the probability that in time t the filament is uncapped for a total time τ . The probability that N monomers have been lost during this time is

$$p(N, t) = \int_0^\infty d\tau u(\tau|t) \mathcal{P}(N, v_{\text{D}}^- \tau), \quad \mathcal{P}(N, x) \equiv x^N e^{-x} / N!, \quad (14)$$

where the Poisson distribution, \mathcal{P} , describes the probability distribution of the number of depolymerized ADP-actin monomers during the total uncapped period. Let us evaluate u by noting that the average value of τ and its second moment are given by

$$\langle \tau \rangle = t S_\infty, \quad \langle \tau^2 \rangle = 2S_\infty \int_0^t dt' \int_{t'}^t S(t'' - t') dt'', \quad (15)$$

for long enough times. Here $S(t)$ is a return probability, namely the probability that the tip is uncapped at time t , given that it was uncapped at $t = 0$, and $S(t) \rightarrow S_\infty$ for $t \rightarrow \infty$. To prove Eq. 15, define $\xi(t''|t')$ to be a random variable that is zero (unity) when the tip is capped (uncapped) at time t'' , given it was uncapped at t' . One has $\langle \tau^2 \rangle = \int_0^t \int_0^t dt' dt'' \langle \xi(t'|0) \xi(t''|0) \rangle = 2 \int_0^t dt' \int_{t'}^t dt'' \langle \xi(t'|0) \rangle \langle \xi(t''|t') \rangle$. Noting that $S(t) = \langle \xi(t|0) \rangle$ one recovers Eq. 15.

Now the exact result for S is (2)

$$S(t) = e^{-(k_{\text{T}}^+ c + v_{\text{T}}^-) t} [I_0(2tx) + y^{-1/2} I_1(2tx) + (1-y) \sum_{j=2}^{\infty} y^{-j/2} I_j(2tx)], \quad y \equiv k_{\text{T}}^+ c / v_{\text{T}}^-, \quad x \equiv (k_{\text{T}}^+ c v_{\text{T}}^-)^{1/2}, \quad (16)$$

where I_j are modified Bessel functions. Using $S_\infty = 1 - c/c_{\text{crit}}$ one obtains for long times $\langle \tau \rangle = t(1 - c/c_{\text{crit}})$ and $\langle \tau^2 \rangle_c = (t/v_{\text{T}}^-)$ where $\langle \rangle_c$ denotes second cumulant. Thus relative fluctuations in τ become small for long times and u becomes Gaussian, $u(\tau|t) \approx \text{const.} \exp[-(\tau - \langle \tau \rangle)^2 / (2 \langle \tau^2 \rangle_c)]$. Substituting u in $p(N, t)$ of Eq. 14 and performing the integration one obtains

$$D_\infty(c) = \begin{cases} (v_{\text{D}}^-/2)[1 + (2v_{\text{D}}^-/v_{\text{T}}^- - 1)c/c_{\text{crit}}] & (c < c_{\text{crit}}) \\ (k_{\text{T}}^+ c + v_{\text{T}}^-)/2 & (c > c_{\text{crit}}) \end{cases}, \quad (17)$$

which is the sawtooth curve plotted in Fig. 6. Notice that D_∞ decreases for smaller concentrations since at $c = 0$ one must recover the Poissonian fluctuations of a pure depolymerization process for which $D_\infty = v_{\text{D}}^-/2$. In Eq. 17, the $c > c_{\text{crit}}$ expression represents the fluctuations of a polymerization process of identical subunits (3) (since in the limit considered here the cap is never lost above c_{crit}).

References

- [1] Bindschadler, M., Osborn, E. A., Dewey, C. F. J. & McGrath, J. L. (2004) *Biophys. J.* **86**, 2720–2739.
- [2] Hill, T. L. (1987) *Linear Aggregation Theory in Cell Biology*. (Springer, New York).
- [3] O’Shaughnessy, B. & Vavylonis, D. (2003) *Eur. Phys. J. E* **12**, 481–496.